

# The k-core as a predictor of structural collapse in mutualistic ecosystems

Flaviano Morone, Gino Del Ferraro and Hernán A. Makse\*

**Collapses of dynamical systems into irrecoverable states are observed in ecosystems, human societies, financial systems and network infrastructures. Despite their widespread occurrence and impact, these events remain largely unpredictable. In searching for the causes for collapse and instability, theoretical investigations have so far been unable to determine quantitatively the influence of the structural features of the network formed by the interacting species. Here, we derive the condition for the stability of a mutualistic ecosystem as a constraint on the strength of the dynamical interactions between species and a topological invariant of the network: the k-core. Our solution predicts that when species located at the maximum k-core of the network go extinct, as a consequence of sufficiently weak interaction strengths, the system will reach the tipping point of its collapse. As a key variable involved in collapse phenomena, monitoring the k-core of the network may prove a powerful method to anticipate catastrophic events in the vast context that stretches from ecological and biological networks to finance.**

A complex dynamical system collapses when a small perturbation in the parameters characterizing the species interactions causes a large-scale extinction of the species in the system<sup>1–12</sup>. The tipping point at which the system suddenly shifts to the irrecoverable state is, for practical purposes, the most important quantity one wishes to know<sup>5,6,13</sup>. It is a function of the dynamical and structural parameters of the system determined by the fixed-point solution of the nonlinear equations describing the system's dynamics<sup>1</sup>. However, the tipping point is hard to determine, due to the difficulties encountered in solving the nonlinear dynamical equations to quantify the dependence of the fixed-point solution on the system parameters and, in particular, on the features of the underlying network of interacting species in the system<sup>1,3,6,8</sup>. Indeed, no exact analytical result exists, so far, that relates the network properties to the fixed points of the dynamical system. Here, we first study numerically the fixed-point equations of a dynamical system of mutualistic species and then derive the analytical solution to compute the tipping point using a logic approximation. Our solution reveals that the root cause of the system collapse is the extinction of species located in the maximum k-core of the network.

The concept of k-core was introduced in social sciences<sup>14</sup> to define network cohesion and then applied in many other contexts<sup>15</sup>, including the robustness of random networks<sup>16</sup>, the structure of the Internet<sup>17,18</sup>, viral spreading in social networks<sup>19</sup>, the large-scale structure of brain networks<sup>20</sup>, and the jamming transition<sup>21</sup>. For a network of interacting species, the k-core is the portion of the network that remains after iteratively removing from the network all species linked to fewer than  $k$  other species (see Fig. 1a,b and Supplementary Section I; refs<sup>14,16</sup>). For a given  $k$ , the subset of species in the k-core consists of the periphery, called the k-shell, and the remaining  $k+1$ -core; therefore, the k-shell is the region of the k-core not included in the  $k+1$ -core (Fig. 1a). Thus, the network has a nested structure of k-cores with increasing k-shells of order  $k_s$ , starting from the periphery of the network or 1-shell,  $k_s=1$ , and its 1-core, which includes all the network (except for isolated nodes). The 1-core contains the 2-core, and so on, up to the innermost core of the network, which is the maximum k-core labelled by the 'k-core number'  $k_{\text{core}}^{\text{max}}$ . The k-core number is a topological invariant of the network<sup>16</sup>.

## Model of a mutualistic ecosystem

We consider complex systems populated by  $N$  interacting species, also referred to as network nodes, whose directed interactions can be graphically portrayed as links in a network via the adjacency matrix  $A_{ij}$  such that  $A_{ij}=1$  if species  $i$  interacts with species  $j$ , and  $A_{ij}=0$  otherwise. In general  $A_{ij} \neq A_{ji}$  for directed networks. The strength of the directed interaction from species  $i$  to species  $j$  is  $\gamma_{ij}$ . In this paper we consider the case of mutualistic ecosystems where organisms of different species cooperate with each other by benefitting from the activities of the other, such as plants and pollinators. These systems are characterized by positive interactions between the species,  $\gamma_{ij} > 0$ . Dynamical systems with positive and negative interactions, such as neuron, gene or predator–prey ecosystems, are out of the scope of the present work and will be treated in a follow-up.

The state of the system is encoded in the multiplet of species densities  $\mathbf{x}(t) \equiv (x_1(t), \dots, x_N(t))$  evolving in time towards a fixed point  $\mathbf{x}^*$ , where  $\mathbf{x}^* = \mathbf{0}$  (ref.<sup>2</sup>). When the species do not interact (that is, for  $\gamma_{ij}=0$ ), each species density changes through time as  $\dot{x}_i(t) = f_i(x_i)$ , and the fixed points are found by solving  $f_i(x_i^*) = 0$  for all  $i$ . When the species interact according to  $\gamma_{ij}$ ,  $x_i(t)$  is influenced by the densities  $x_j(t)$  of the species linked to it in the network of interactions. Although these interactions are generally complex, it is widely recognized that they saturate when the density of interacting species increases<sup>22–27</sup>. This occurs in mutualistic interactions between species in ecosystems, for which the benefit accorded by one species to another saturates to a limiting value<sup>22–25</sup>. In biology, the expression level of gene products are modelled by Hill or sigmoidal response functions which saturate at high concentrations of the interacting gene (Supplementary Section II)<sup>26</sup>. Enzymatic reactions are also modelled by Hill functions in the Michaelis–Menten equation<sup>26</sup> and firing rates of neurons saturate at high membrane potentials via sigmoidal functions<sup>27,28</sup>.

In the following, we treat explicitly the paradigmatic case of dynamical systems of ecological mutualistic networks, but the results we obtain hold true for the larger class of nonlinear systems where a Hill or sigmoidal function models the interactions. A network of mutualistic species describes a system of symbionts obligated to each other because they cannot survive independently<sup>22,23,25</sup>; for example, an ecosystem of plants and pollinators (Fig. 1b).

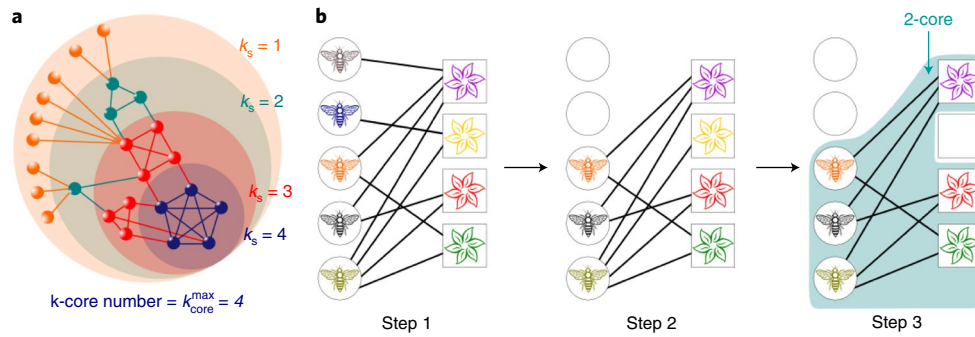


**Fig. 1 | k-core structure of a mutualistic network.** **a**, Schematic representation of a network as successive enclosed  $k$ -cores, which are the largest subgraphs of the network where each species is connected at least to  $k$  other species. Species are classified by their  $k$ -shell  $k_s$ , which is the value  $k$  of the higher-order  $k$ -core to which they belong. The maximum value  $k_{\text{core}}^{\text{max}}$  attainable by  $k_s$  defines the  $k$ -core number of the entire network ( $k_{\text{core}}^{\text{max}} = 4$  in this case). **b**, Schematic example of a plant-pollinator mutualistic bipartite network and the pruning process for extracting the 2-core. At Step 1 the full network is a 1-core. Then, we remove all species with degree 1, consisting of the two pollinators in the upper left circles (Step 2). These removals produce a new one-degree species, which is the yellow plant on the right in Step 2. Thus, at Step 3, we remove this plant as well. The network at Step 3 consists of species of degree 2 or greater, so the pruning process stops and the result is the 2-core, while the three removed species constitute the  $k_s = 1$  shell. Image credit: Bee vector drawing.eps from 365PSD.com.

The dynamics of species densities,  $x_i(t)$ , interacting via the network  $A_{ij}$  with directed and positive interaction strengths  $\gamma_{ij}$ , is described by the following set of nonlinear differential equations<sup>22–25,29</sup>:

$$\dot{x}_i(t) = -dx_i - sx_i^2 + \sum_{j=1}^N A_{ij}\gamma_{ij} \frac{x_i x_j}{\alpha + \sum_{k=1}^N A_{ik}x_k}, i \in \{1, \dots, N\} \quad (1)$$

Here  $d > 0$  is the death rate of the species,  $s > 0$  is the self-limitation parameter modelling the intraspecific competition that limits a species' growth once  $x_i$  exceeds a certain value,  $\alpha$  is the half-saturation constant, and  $\gamma_{ij} > 0$  is the mutualistic interaction strength between species  $i$  and  $j$ , characterizing the strength of the nonlinear interaction term. The dynamical parameters ( $\{\gamma_{ij}\}$ ,  $d$ ,  $s$ ,  $\alpha$ ) have been extensively discussed in the literature<sup>22–25,29</sup>. The network is bipartite between, for example, plants and pollinators (Fig. 1b). Our goal is to bridge the gap from structure to dynamics by obtaining the fixed-point solution of dynamical equations to predict the tipping point of collapse in terms of a feature of the network.

### Numerical analysis of the ecosystem collapse

We start by performing a numerical study of the tipping point of the system (details in Methods and Supplementary Section III), then we elaborate our analytical solution based on approximations supported by the numerical evidence. Figure 2b–f shows the numerical solution of equation (1) for different parameters on a real plant-pollinator mutualistic network from the Chilean Andes obtained from ref.<sup>30</sup> (Net 10 in Supplementary Table 1). We plot the fixed-point average density (properly rescaled)  $\langle x^* \rangle = N^{-1} \sum_i x_i^*$  as a function of  $K_\gamma = \frac{\alpha s (\gamma + d)}{(\gamma - d)^2}$ , which is the main control parameter that determines the collapse of the system according to the theoretical solution in equation (4). Here  $\gamma$  is the average interaction strength and  $K_\gamma \approx 1/\gamma$ , since  $d \ll \gamma$ .

By increasing  $K_\gamma$  or, analogously, decreasing the interactions  $\gamma$ , we find that for all the numerical ecosystems in Fig. 2 there exists a point of collapse at a given critical value  $K_\gamma^c$  (or analogously  $\gamma_c$ ), which is the tipping point of the ecosystem. This collapse is exemplified by the transition from a non-zero fixed point  $\langle x^* \rangle \neq 0$  for  $K_\gamma < K_\gamma^c$ , where the species are alive, to a zero fixed point  $\mathbf{x}^* = \mathbf{0}$  for  $K_\gamma > K_\gamma^c$  that corresponds to the extinction of all species<sup>8,23,25,29,31</sup>.

The collapsed phase corresponds to the trivial fixed point of equation (1),  $\mathbf{x}^* = \mathbf{0}$ . The decrease of the interaction  $\gamma$  that drives the system to collapse for  $\gamma < \gamma_c$  could be caused, for example, by external global conditions such as changes in environmental conditions due

to global climate change. These global changes produce shifts in phenology, and hence changes in the interaction strength  $\gamma$  that affect all species<sup>5,6</sup>. The question is then how to predict this tipping point.

### Analytical solution of the ecosystem collapse

We first show that the fixed-point equations for this system can be written in terms of the Hill function<sup>23,26</sup>. We consider a system with  $\gamma_{ij} = \gamma$  (see Methods) and make a change of variables to the reduced density:

$$y_i^* = \frac{s}{\gamma - d} \sum_{j=1}^N A_{ij} x_j^* \quad (2)$$

whereby the fixed-point equations can be written using a sum of Hill functions of the form  $H_1(x, T) = x/(T + x)$ , where  $T > 0$  is the half-saturation constant<sup>23,26</sup> (details in Supplementary Section V):

$$y_i^* = \sum_{j=1}^N A_{ij} H_1 \left( y_j^* - \frac{\alpha ds}{(\gamma - d)^2}, \frac{\alpha \gamma s}{(\gamma - d)^2} \right) \quad (3)$$

The Hill function  $H_1$  is the first of a family of response functions parametrized by the Hill coefficient  $n$  as  $H_n(x, T) = x^n/(T^n + x^n)$ , where  $n$  characterizes the degree of cooperativity among the interacting species<sup>26,32</sup>. This particular interaction term in equation (1) is not crucial for the solution of the problem: any saturating sigmoidal-like function will lead to the  $k$ -core collapse of the dynamical system (Supplementary Section II).

A widely used approximation to treat these systems analytically involves the logic approximation of the Hill function as proposed by Kauffman<sup>33</sup> to describe genetic Boolean networks<sup>34</sup>. This approximation assumes  $n \rightarrow \infty$  and replaces the interaction function by a logic ON and OFF switch according to whether the input  $x$  is above the threshold  $T$  or below, respectively. That is, it replaces  $H_1$  by  $H_1(x, T) \approx \Theta(x - T)$ , where the Heaviside function  $\Theta(x) = 1$  if  $x > 0$  and zero otherwise. Both the continuous description for finite  $n$  and its Boolean-logic approximation for  $n \rightarrow \infty$  are also widely used to describe artificial and real neural networks<sup>27</sup>. Inspired by these works<sup>26,27,33,34</sup>, we apply the logic approximation to equation (3) to solve the model analytically (Supplementary Section IV systematically investigates numerically the limit of validity of the logic approximation).

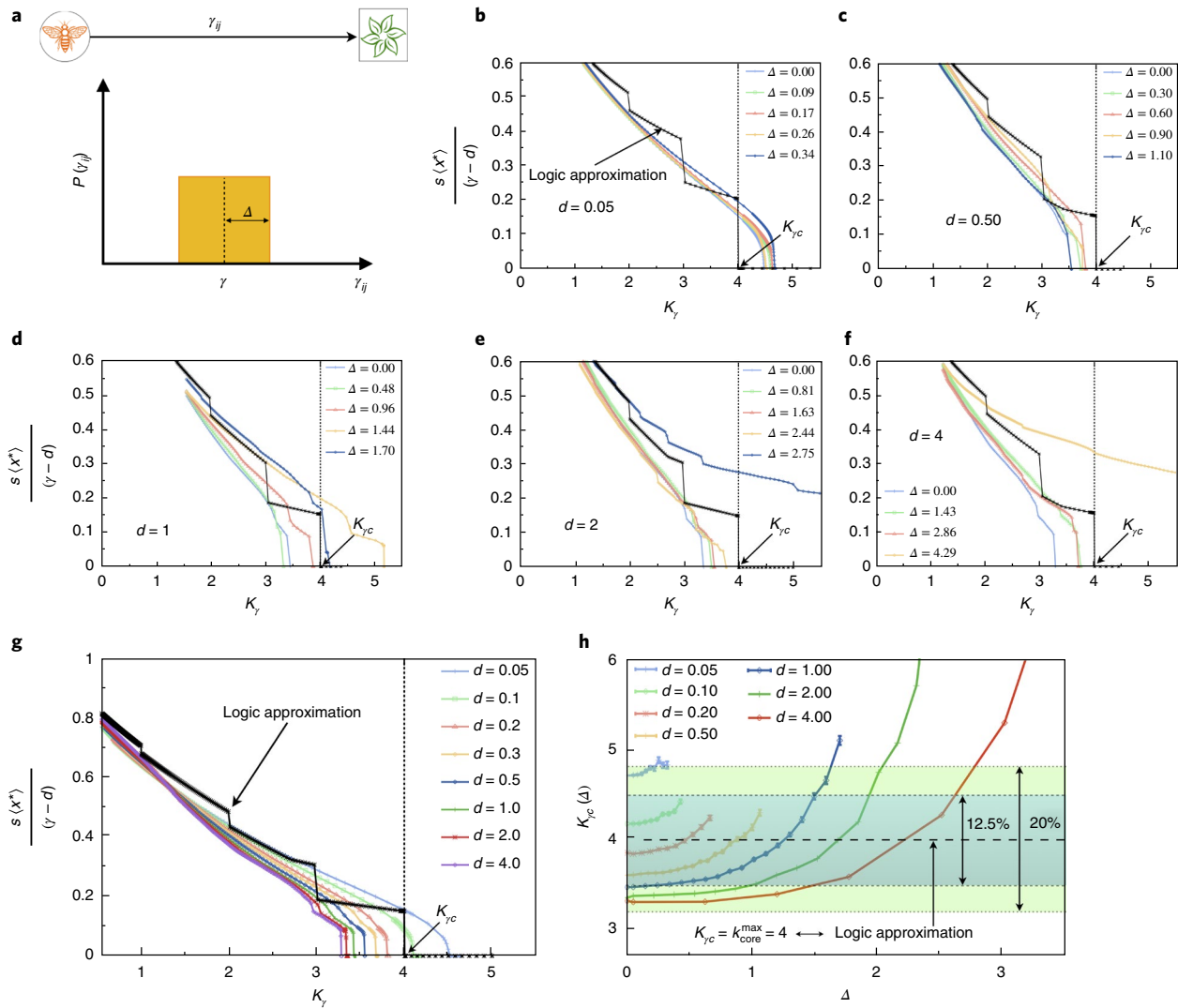


**Fig. 2 | Numerical solution to the fixed-point equations in weighted and directed networks.** **a**, Definition of the directed interaction strength  $\gamma_{ij}$  from a plant  $i$  to a pollinator  $j$ . The interaction strengths  $\gamma_{ij}$  are i.i.d. random variables drawn from a uniform distribution  $P(\gamma_{ij})$  with mean  $\gamma$  and width  $\Delta$ . **b**, Fixed-point average density (properly rescaled)  $\langle x^* \rangle = N^{-1} \sum_i x_i^*$  as a function of  $K_\gamma = \frac{as(\gamma+d)}{(\gamma-d)^2}$  (which is proportional to the inverse average interaction strength  $1/\gamma$ , for small  $d$ ) for the network of a plant-pollinator mutualistic ecosystem located in the Chilean Andes<sup>30</sup> (Net 10 in Supplementary Table 1), obtained by solving numerically equation (1) using a fourth-order Runge-Kutta algorithm. The death rate is  $d=0.05$ . Each curve is computed using a different sample of interaction strengths  $\{\gamma_{ij}\}$  with a different width  $\Delta$  as defined in **a**. For  $\Delta=0$ , all  $\gamma_{ij}$  are equal. The largest value  $\Delta=0.34$  corresponds to the maximal possible width compatible with mutualistic interactions—that is, such that all  $\gamma_{ij}$  are non-negative (details of the numerical simulations in Supplementary Section III). We also plot the analytical solution obtained through the logic approximation (black line). **c-f**, Same as in **b**, but using death rates  $d=0.5, 1, 2, 4$ , respectively, together with the logic approximation solution. **g**, Fixed-point average density  $\langle x^* \rangle$  properly rescaled as a function of the threshold  $K_\gamma$  for several values of  $d$  and  $\Delta=0$ . For comparison, the analytical solution obtained through the logic approximation—that is, the solution of equation (4), or equivalently equation (6)—is plotted as a function of  $\langle x^* \rangle$  (black line). The theoretical prediction of the critical value  $K_{\gamma_c} = k_{\text{core}}^{\text{max}}$  is shown in panels **b-g** with a black arrow. **h**, Critical average interaction strength  $K_{\gamma_c}(\Delta)$  as a function of the width  $\Delta$  for different values of  $d \in [0.05, 4.0]$  obtained from **b-f**. Each curve ends at a given value of  $\Delta$ , which depends on  $d$ , representing the maximum admissible width compatible with mutualistic interactions  $\gamma_{ij} \geq 0$ . Deviations of more than 20% from the theoretical prediction given by the logic approximation are found only for large  $d$  (that is  $d > 1$ ) and distribution width  $\Delta > 1.5$  (outside the green shaded band). For values of  $d$  of the order of  $[0.1-0.3]$ , which are the values found in the literature<sup>23,25</sup>, the theoretical predictions of the logic approximation are even more accurate and in agreement with the numerical simulations of the  $n=1$  model within 12.5%, for any  $\Delta$  (blue shaded band).

By using the logic approximation of the Hill function<sup>26,27,33,34</sup> (that is  $H(x, T) \rightarrow \Theta(x - T)$ ), the fixed-point equations can be recast in the following analytically tractable form:

$$y_i^* = \sum_{j=1}^N A_{ij} \Theta(y_j^* - K_\gamma) \quad (4)$$

$$K_\gamma = \frac{as(\gamma+d)}{(\gamma-d)^2}$$

where  $K_\gamma$  is the threshold on the mutualistic benefit; the subscript emphasizes its main dependence on  $\gamma$ ,  $K_\gamma \propto 1/\gamma$  (Fig. 3a) since  $d \ll \gamma$ . Concretely,  $K_\gamma$  is the threshold of the  $\Theta$ -function in equation (4), which allows species  $i$  to benefit from mutualistic interactions with species  $j$  only when their densities  $y_j^*$  are greater than  $K_\gamma$ . Weak interactions  $\gamma$  correspond to large thresholds  $K_\gamma$ , which, by inhibiting the benefits  $y_j^*$  conferred by species  $j$  to  $i$ , produce small values of  $y_i^*$ . Thus, if  $\gamma$  falls below the critical value  $\gamma_c$ , no mutualistic benefit is exchanged among species since the corresponding critical threshold,

$$K_{\gamma_c} = \frac{\alpha s(\gamma_c + d)}{(\gamma_c - d)^2} \quad (5)$$

is too high, and the entire system collapses via a catastrophic transition to the state  $\mathbf{x}^* = \mathbf{0}$  (Fig. 3a), as shown numerically in Fig. 2b–f.

Next we show that the critical interaction strength for collapse,  $\gamma_c$  (or  $K_{\gamma_c}$ ), is determined by the maximum k-core of the network  $k_{\text{core}}^{\text{max}}$ . The reduced density  $y_i^*$  assumes only integer values in the set  $y_i^* \in \{1, \dots, k_i\}$ , where  $k_i$  is the degree of, or number of species interacting with, species  $i$ . Therefore, to solve for  $y_i^*$  at a given threshold  $K_{\gamma}$ , we remove all species  $j$  with degree  $k_j < K_{\gamma}$  from equation (4), since these species give zero contribution to the right-hand side of equation (4), and we solve only for the remaining species. The procedure is explained graphically in Fig. 3b for a simple ecosystem with a maximum 2-core and interaction strength that could be anywhere between  $1 < K_{\gamma} < 2$ , and in Supplementary Section V A, for fully connected networks of 2, 3 and 4 species.

After these first removals are done (Step 1 in Fig. 3b), the species left in the network have smaller degree  $k'_j$ , and we perform a new wave of removals of species  $j'$  if  $k'_j < K_{\gamma}$  (Step 2 in Fig. 3b). This pruning process stops when the degree of each remaining species is greater than  $K_{\gamma}$ . The process we just described is precisely the algorithm for extracting the  $K_{\gamma}$ -core of the network<sup>14,16,19</sup>, as explained in Fig. 1b: iteratively removing all species from the network with degree  $k < \lceil K_{\gamma} \rceil$ , where  $\lceil \cdot \rceil$  denotes the ceiling function. Thus, the nodes remaining at the end of this pruning process, if any, form a  $K_{\gamma}$ -core by construction, as shown in Step 3 of Fig. 3b. Since  $y_i^*$  in equation (4) measures the number of links of species  $i$  to this remaining  $K_{\gamma}$ -core, we find the nontrivial fixed-point solution for the species belonging to this  $K_{\gamma}$ -core as (see Fig. 3b Step 3):

$$y_i^* = \text{number of links of species } i \text{ to species in the } K_{\gamma} \text{-core} \quad (6)$$

$$\equiv \mathcal{N}_i(K_{\gamma})$$

Equation (6) remains valid also for the species placed outside the  $K_{\gamma}$ -core, since the only nonzero benefits they receive come from species inside the  $K_{\gamma}$ -core (Fig. 3c). Indeed, for a species  $i$  outside the  $K_{\gamma}$ -core,  $y_i^*$  may be nonzero only if species  $i$  interacts with at least one species inside the  $K_{\gamma}$ -core. However, those species for which  $0 < y_i^* < \lceil K_{\gamma} \rceil$  have no influence in the ecosystem, meaning that their disappearance does not change the density of any other species. In practice, they are commensalists rather than symbionts, that benefit from the species located in the  $K_{\gamma}$ -core without benefitting or damaging them, as seen in Fig. 3c.

### The maximum k-core of a network predicts tipping points

Equation (6) reveals how the dynamics is intertwined with the network structure through the number of links to the  $K_{\gamma}$ -core,  $\mathcal{N}_i(K_{\gamma})$ . Indeed, when these links disappear, the system collapses. Since the densities must be positive by definition,  $x_i^* > 0$  ( $x_i^*$  is obtained from equation (6) by a change of variables, see Supplementary Equation (24)), hence  $y_i^*$  must also be positive. Then, we must have  $\mathcal{N}_i(K_{\gamma}) > 0$ . However, this condition cannot be satisfied by any species  $i$  if  $K_{\gamma} > k_{\text{core}}^{\text{max}}$ , because when the threshold  $K_{\gamma}$  in equation (4) is greater than the maximum k-core of the network, the number of links to the  $K_{\gamma}$ -core is, by definition, zero (that is,  $\mathcal{N}_i(K_{\gamma} > k_{\text{core}}^{\text{max}}) = 0$ ). As a consequence, if  $\gamma$  is reduced to the point that  $K_{\gamma}$  is slightly greater than the maximum k-core  $k_{\text{core}}^{\text{max}}$ , so that  $K_{\gamma} > k_{\text{core}}^{\text{max}}$ , the system collapses to the state  $x_i^* = 0$ , where the species are extinct. The critical value  $\gamma_c$  at this tipping point of collapse is predicted as:

$$K_{\gamma_c} = k_{\text{core}}^{\text{max}} \rightarrow \alpha s \frac{(\gamma_c + d)}{(\gamma_c - d)^2} = k_{\text{core}}^{\text{max}} \quad (7)$$

which represents our main result relating the dynamical parameters at the tipping point to a global topological network property.

We confirm the main theoretical result of equation (7) with a numerical simulation using the same mutualistic network of Fig. 2 (Net 10 in Supplementary Table 1, Fig. 4a shows its k-shell structure). Figure 4b shows the fixed-point average density ( $x^*$ ) for this system, which confirms that the collapse of the ecosystem occurs when  $K_{\gamma_c}$  satisfies the critical condition in equation (7). That is, the system collapses at  $K_{\gamma_c} = 4$ , which corresponds to the maximum k-core for this network,  $k_{\text{core}}^{\text{max}} = 4$  (Fig. 4a). We also compare the logic approximation (black curve) to the numerical solutions in Fig. 2b–f, as well as Fig. 2g, which corresponds to the case where  $\Delta = 0$ . Figure 2h plots the numerical tipping point  $K_{\gamma_c}$  compared to the k-core prediction for this network,  $k_{\text{core}}^{\text{max}} = 4$ . We find that the logic approximation captures well the tipping point of the system across realistic values of death rate parameters  $d \in [0.1-0.3]$ <sup>23,25</sup> (further examinations are provided in Supplementary Section VI).

As the interaction strength decreases (so  $K_{\gamma}$  increases) due to external global conditions, the system suffers a series of partial collapses, characterized by the sharp drops in the species density shown in Fig. 4b, at successive precise integer values of  $K_{\gamma}$  equal to the index  $k_s$  of each k-shell. This occurs until the species in the maximum k-core at  $k_{\text{core}}^{\text{max}} = 4$  go extinct, with the concomitant collapse of the entire network. Therefore, as the strength of mutualistic interaction  $\gamma$  decreases, the species in the outer k-shells (the ‘leaves’ in the network) go extinct first, whereas species in the innermost k-core survive up to the tipping point of total collapse (insets in Fig. 4b). As a consequence, equation (7) can be used as a warning signal for the proximity of the system to the tipping point by measuring independently the dynamical parameters and the k-core number of the network.

In Supplementary Section VI F we compare the prediction of the tipping point of the system made by  $k_{\text{core}}^{\text{max}}$  to the prediction of collapse made by other metrics, such as nestedness<sup>35,36</sup>, spectral radius<sup>37</sup>, and connectance (average degree). Supplementary Fig. 4 shows the result of this comparison. Overall, the metrics which are related to  $k_{\text{core}}^{\text{max}}$  via mathematical bounds—for example, the spectral radius ( $\rho \geq k_{\text{core}}^{\text{max}}$ <sup>38</sup>) and the connectance—are also good predictors of the tipping point when these bounds are saturated. However, in more general conditions, far from saturated bounds,  $k_{\text{core}}^{\text{max}}$  remains the metric which theoretically predicts the collapse of the system.

### Stability analysis and phase diagram of system feasibility

Once we have the solution (equation (6)) to the fixed-point equations, we can study its local stability, which is controlled by the stability matrix  $\mathcal{M}_{ij} = \frac{\partial x_i}{\partial x_j} \Big|_{\mathbf{x}^*}$ . Indeed, stability theory has been at

the core of the ecosystem literature since May<sup>1</sup> posed the question whether a large ecosystem would become stable or unstable (see below).

A fixed-point solution (equation (6)) is locally stable if all the eigenvalues  $\lambda_i^{\mathcal{M}}$  of the stability matrix  $\widehat{\mathcal{M}}$  have a negative real part<sup>1</sup>. These eigenvalues can be calculated analytically in our model. We find (see Supplementary Section VII):

$$\lambda_i^{\mathcal{M}} = -\gamma \frac{\mathcal{N}_i(K_{\gamma})}{K_{\gamma} + \mathcal{N}_i(K_{\gamma})}, \quad i = 1, \dots, N \quad (8)$$

which are, in fact, all negative. Therefore our solution, if it exists, is always stable. This result has important consequences, as we show next.

Interestingly, the largest and thus most critical eigenvalue  $\lambda_{\text{max}}^{\mathcal{M}}$  is the one corresponding to the commensalist species  $i$  with the minimal number of links  $\mathcal{N}_i$  to the symbionts located in the

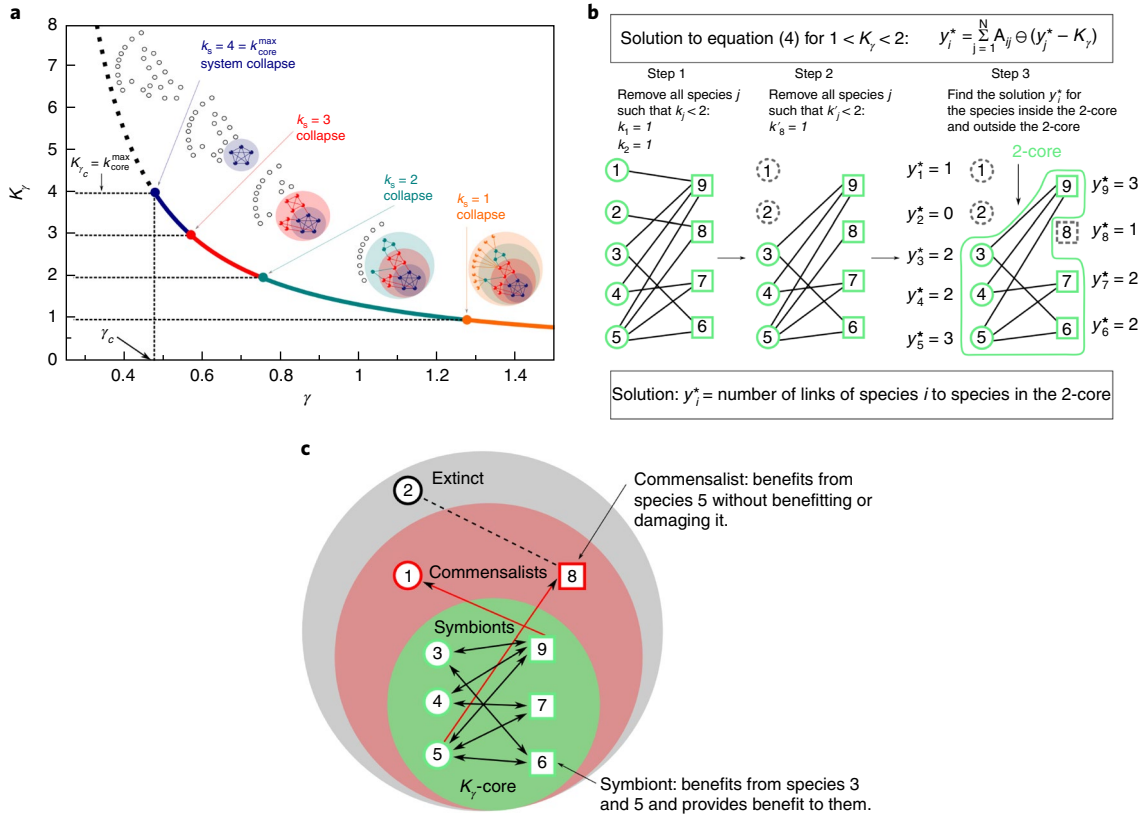


**Fig. 3 | Solution scheme for the fixed point equations (4).** **a**, Threshold  $K_\gamma$  as a function of the interaction strength  $\gamma$  for the network shown in Fig. 1a. For large  $\gamma$  such that  $K_\gamma < 1$ , all species in the network provide their mutualistic benefit to the species they interact with. If  $\gamma$  is reduced such that  $K_\gamma$  is slightly above 1, none of the species with  $k_s = 1$  can confer their benefits to the others, while the species in the 2-core keep providing their benefit. When  $\gamma$  is further reduced, so that  $K_\gamma$  becomes slightly larger than 2, the species with  $k_s = 2$  also cease to provide their benefit, while the species in the 3-core are still able to dispense theirs. Further reducing  $\gamma$  also inhibits the mutualistic benefit from species in the 3-shell, and eventually causes the threshold  $K_\gamma$  to surpass the value of the  $k$ -core number of the network  $K_\gamma > k_{\text{core}}^{\text{max}} = 4$ , at which point the entire system collapses, since no remaining species can provide mutualistic benefits. This series of collapses results in the staircase shape plot of the species density shown in Fig. 4b. **b**, To explain our solution we consider a simple ecosystem network that contains a 2-core and species with interaction strength  $k_j$  in the range  $1 < K_\gamma < 2$ . Step 1: we consider the bipartite network with all species present. Step 2: we remove from the network all species  $j$  having degree  $k_j < K_\gamma$ , since the corresponding variables  $y_j^*$  give zero contribution to the right-hand side of equation (4). In this case we remove the species 1 and 2, since  $k_1, k_2 < K_\gamma = 2$ . Step 3: after these first removals, the species left in the network have smaller degree  $k'_j$ , and we perform a new wave of removals of species  $j'$  if  $k'_j < K_\gamma = 2$ . So we remove species 8, since  $k'_8 < 2$ . At this point the pruning process stops, since the degree of the remaining species is greater than or equal to 2. These remaining species 3, 4, 5, 6, 7 and 9 form the 2-core of the network. Since  $y_i^*$  in equation (4) measures the number of links to this remaining 2-core, the solution  $y_i^*$  for the species inside the 2-core is:  $y_3^* = 2, y_4^* = 2, y_5^* = 3, y_6^* = 2, y_7^* = 2, y_9^* = 3$ . Step 4: once the solution for the variables inside the 2-core has been found, we can add back the removed species and determine the full fixed-point solution. In this case we add back the species 1, 2 and 8. To this end, it is sufficient to notice that, even for the species placed outside the 2-core,  $y_i^*$  in equation (4) still measures the number of links to species inside the 2-core. Therefore, since species 1 and 8 are connected to exactly one species in the 2-core, we find  $y_1^* = 1$  and  $y_8^* = 1$ . In contrast to species inside the 2-core, species 1 and 8 have no influence on the system, meaning that their removal does not change the value of any other variable. **c**, In ecological terms, species 1 and 8 are commensalists, as shown schematically, as opposed to the true symbionts living in the 2-core, because they receive a benefit from the species in the 2-core but provide no benefit in return. Lastly, for species 2, we find  $y_2^* = 0$ , since this species has no links to species in the 2-core. Hence it represents an extinct species. This exact solution is corroborated numerically in Fig. 4b.

$K_\gamma$ -core (Fig. 3c). The most critical species—that is, species most exposed to extinction—are commensalists with a single link to the  $K_\gamma$ -core with  $\lambda_{\text{max}}^M = -\gamma / (K_\gamma + 1)$ . As the system approaches its collapse, the commensalists with the fewest number of links to the  $K_\gamma$ -core go extinct first. Such a dynamics is clearly seen in the sketches of Fig. 3a and the network panels of the numerical solution in Fig. 4b.

Thus, our solution predicts that the system’s approach to the tipping point of collapse is signalled by an increase of commensalist species at the outer shells, and a reduction of symbionts at the inner cores. From equation (8) we also conclude that when  $K_\gamma > k_{\text{core}}^{\text{max}}$ , all the eigenvalues vanish, thus the feasible fixed point becomes unstable (and also unfeasible), with the concomitant extinction of

all species. This confirms the tipping point equation (7) derived above from the existence of the feasible nontrivial solution.

These considerations lead to the phase diagram of feasible and stable mutualistic ecosystems depicted in Fig. 5a in the space  $(K_\gamma, k_{\text{core}}^{\text{max}})$ . The phase diagram features the predicted ‘tipping line’ of instability defined by the condition in equation (7), which separates the feasible-stable phase:

$$K_\gamma < k_{\text{core}}^{\text{max}} \quad (9)$$

(condition of existence of the feasible - stable state)

from the collapsed phase:

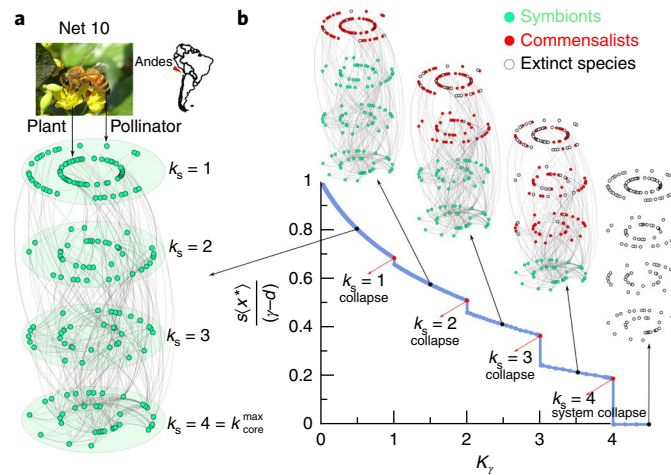


**Fig. 4 | Collapse of a plant-pollinator mutualistic network and the tipping line of the mutualistic ecosystem.** **a**, A bipartite mutualistic network of a plant-pollinator ecosystem located in the Chilean Andes<sup>30</sup> (Net 10 in Supplementary Table 1). The network is formed by four pairs of concentric rings. Each pair of rings contains species with the same k-shell  $k_s$ , ranging from one to four (analogous to Figs. 1a and 3a). The innermost core is at  $k_{\text{core}}^{\text{max}} = 4$ . Species in the inner rings of each k-shell represent the plants, and species in the outer rings represent the pollinators. **b**, Fixed-point average density (properly rescaled)  $\langle x^* \rangle = N^{-1} \sum_i x_i^*$  as a function of the threshold  $K_\gamma$  (equation (4)), for the mutualistic network in **a**, obtained by numerical integration (see Supplementary Section III). For  $K_\gamma < 1$ , all species are extant and provide their mutualistic benefit to the species they are linked to in the interaction network (extant species, green solid symbols). When  $K_\gamma$  is above 1, the species in the outer k-shell  $k_s = 1$  can no longer provide their benefit, since  $K_\gamma > k_s$ . However, a species with  $k_s = 1$  can still benefit from species in the higher shells  $k_s > 1$ , and if it benefits from at least one of them, it is still extant (red symbols), otherwise it is extinct (open circles). The species in red are termed commensalists because they receive a benefit from other species, but provide no benefit in return. Increasing the threshold further causes more extant species to become commensalists or to go extinct whenever  $K_\gamma$  rises above integer values of the successive k-shell. Finally, when  $K_\gamma$  becomes larger than  $k_{\text{core}}^{\text{max}} = 4$ , there are no remaining species that can provide a mutualistic benefit, and the whole system suddenly collapses. Image credit: copyright, Guglielmo Castagnoli (**a**).

$$K_\gamma > k_{\text{core}}^{\text{max}} \quad (\text{condition of collapsed state}) \quad (10)$$

We test this phase diagram by plotting the values of  $(K_\gamma, k_{\text{core}}^{\text{max}})$  obtained from real mutualistic networks of plant-pollinator and plant-seed dispersers<sup>3,25</sup> (see Fig. 5a, Supplementary Table 1 and Supplementary Section IV). All real mutualistic ecosystems lie in the feasible-stable region situated above the tipping line, in agreement with the theory.

This conclusion contrasts with the prediction obtained by approximative linear stability methods introduced by May<sup>1</sup> based on Wigner's semicircle law and frequently used in the literature<sup>7,10</sup>. This approach considers a linear model of species interactions rather than the sigmoidal Hill function. The stability matrix is then  $\mathcal{M}'_{ij} = -\delta_{ij} + A_{ij} / K_\gamma$ , and, assuming a random adjacency matrix  $A_{ij}$ , is computed with random matrix theory<sup>1,7</sup>. The stability condition on the negativity of the real part of the most critical eigenvalue of  $\mathcal{M}'_{ij}$  is now given by  $\lambda_{\text{max}}^A < K_\gamma$ , where  $\lambda_{\text{max}}^A$  is the largest eigenvalue of  $A_{ij}$  (see Supplementary Section VII A and ref. <sup>1</sup>). The condition  $\lambda_{\text{max}}^A < K_\gamma$  leads to the May's diversity-stability paradox<sup>1</sup>, by which an ecosystem would become unstable on increasing the diversity of the species. This prediction is valid for any type of ecosystem, and in particular for a mutualistic ecosystem, leading to the paradoxical result that cooperation destabilizes the ecosystem. This paradox arises because  $\lambda_{\text{max}}^A$  increases with the number of species in the ecosystem<sup>1</sup> and therefore, diversity, as measured by the number of species, has a destabilizing effect.

In contrast, our nonlinear theory predicts the opposite result. First, we predict that mutualistic interactions are beneficial for the ecosystem: for a given network structure (fixed  $k_{\text{core}}^{\text{max}}$ ), systems with larger  $\gamma$  tend to be more robust since condition in equation (9) is easier to satisfy. Second, as the diversity of the ecosystem, measured as number of symbionts in the maximum core  $k_{\text{core}}^{\text{max}}$ , increases, the

value  $k_{\text{core}}^{\text{max}}$  increases, hence the condition equation (9) is also easier to satisfy in this case. Therefore, diversity of symbionts at the maximum core of the network increases the stability of the system.

Thus, we show that the analytical solution of the nonlinear model resolves the long-standing diversity-stability paradox<sup>1</sup> in mutualistic ecosystems by introducing a new principle of stability. This principle states that the more symbionts there are in the maximum core of the network, the higher the robustness. Thus, diversity, mutualism and cooperation stabilizes the ecosystem rather than the opposite, as paradoxically proposed in ref. <sup>1</sup>. Our results highlight the importance of considering the exact stability analysis of the nonlinear model equation (1) instead of the linear model when reaching conclusions about the stability of ecosystems. Indeed, studies of the microbiome<sup>10</sup> based on the linear model and Wigner's semicircle law have concluded that cooperating networks of microbes in the human gut are often unstable, in contrast to empirical evidence.

## Summary

We presented an analytic solution of the tipping point for a nonlinear model of mutualistic dynamical systems in terms of a topological invariant of the network, the k-core number. The k-core structure of the network privileges the species at the inner k-core, which are 'keystone species'<sup>39</sup> like the plant *Angelica pubescens* in Net 2 (Fig. 5b). These keystone species are analogous to 'influencers' in social networks<sup>19,40</sup> that guarantee the integrity of the entire ecosystem. Therefore, species at the innermost core should be protected first for the sake of the whole ecosystem.

Since our theoretical results are applicable to a large class of systems governed by nonlinear Hill, logistic or sigmoidal interactions, the conclusions could be equally applicable to other complex systems. Drawing analogies from financial and banking ecosystems<sup>11,12</sup>, to neural circuitry<sup>27,28</sup>, microbial ecosystems<sup>10,41</sup>, and gene regulatory networks<sup>26,33,34</sup>, our results provide the way to avoid systemic risks built in these systems by protecting the system's vital core.

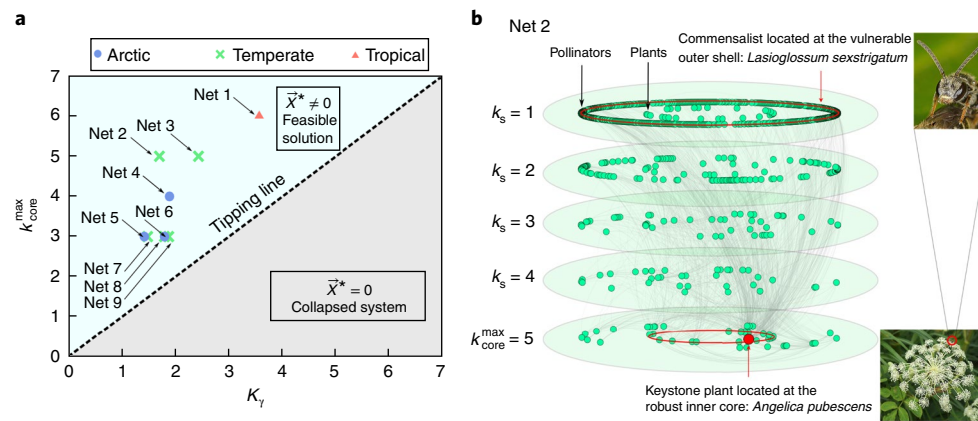


**Fig. 5 | Phase diagram of ecosystem stability.** **a**, Predicted phase diagram for  $k$ -core number  $k_{\text{core}}^{\text{max}}$  versus  $K_y$  for nine empirical mutualistic networks (Net 1–9 in Supplementary Table 1) corresponding to ecosystems at different latitudes: Arctic (blue point), Temperate (green cross) and Tropical (red triangle). All the networks lie in the stable feasible region predicted by equation (9),  $k_{\text{core}}^{\text{max}} > K_y$  (that is, above the tipping line defined by  $k_{\text{core}}^{\text{max}} = K_y$ ). **b**, Network structure for Net 2, the plant–pollinator ecosystem in Japan from ref. 42. Species are arranged in the same way as in **a** (that is, ordered by increasing  $k$ -shell number  $k_s$  from top to bottom, with plants in the inner circles and pollinators in the outer circles). From this graphical representation an interesting structure emerges. Many pollinators in the outer shell  $k_s = 1$  interact with a single keystone plant species, the *Angelica pubescens*, located in the innermost core of the network, and therefore quite stable to external changes, since the inner core is the most stable core in the ecosystem. In contrast, there are far fewer plant species in the outer shell ( $k_s = 1$ ) interacting with just a single pollinator in the inner core ( $k_{\text{core}}^{\text{max}}$ ). Plants tend to populate the more robust inner  $k$ -shells, whereas pollinators concentrate more in the low  $k$ -shells (that is, the upper levels). This result hints that plants are more dependent on the survival of many pollinators than vice versa, a conclusion stemming directly from the  $k$ -core organization of the ecological network. Image credit: copyright, plant, H. Zell (**b**); insect, Ab Baas (**b**).

## Online content

Any methods, additional references, Nature Research reporting summaries, source data, statements of data availability and associated accession codes are available at <https://doi.org/10.1038/s41567-018-0304-8>.

Received: 27 July 2017; Accepted: 4 September 2018;

Published online: 22 October 2018

## References

- May, R. M. Will a large complex system be stable? *Nature* **238**, 413–414 (1972).
- Strogatz, S. *Nonlinear Dynamics and Chaos: With Applications to Physics, Biology, Chemistry, and Engineering* (Westview Press, 2000).
- Caldarelli, G. & Vespignani, A. *Large Scale Structure and Dynamics of Complex Networks: From Information Technology to Finance and Natural Science* (World Scientific, Singapore, 2007).
- Buldyrev, S. V., Parshani, R., Paul, G., Stanley, H. E. & Havlin, S. Catastrophic cascade of failures in interdependent networks. *Nature* **464**, 1025–1028 (2010).
- Scheffer, M. et al. Early-warning signals for critical transitions. *Nature* **461**, 53–59 (2009).
- Scheffer, M. et al. Anticipating critical transitions. *Science* **338**, 344–348 (2012).
- Allesina, S. & Tang, S. Stability criteria for complex ecosystems. *Nature* **483**, 205–208 (2012).
- Gao, J., Barzel, B. & Barabási, A.-L. Universal resilience patterns in complex networks. *Nature* **530**, 307–312 (2016).
- Bascompte, J., Jordano, P. & Olesen, J. M. Asymmetric coevolutionary networks facilitate biodiversity maintenance. *Science* **312**, 431–433 (2006).
- Coyte, K. Z., Schluter, J. & Foster, K. R. The ecology of the microbiome: networks, competition, and stability. *Science* **350**, 663–666 (2015).
- Haldane, A. G. & May, R. M. Systemic risk in banking ecosystems. *Nature* **469**, 351–355 (2011).
- Battiston, S., Caldarelli, G., Georg, C.-P., May, R. M. & Stiglitz, J. Complex derivatives. *Nat. Phys.* **9**, 123–125 (2013).
- Dai, L., Vorsele, D., Korolev, K. S. & Gore, J. Generic indicators for loss of resilience before a tipping point leading to population collapse. *Science* **336**, 1175–1177 (2012).
- Seidman, S. B. Network structure and minimum degree. *Soc. Networks* **5**, 269–287 (1983).
- Pittel, B., Spencer, J. & Wormald, N. Sudden emergence of a giant  $k$ -core in a random graph. *J. Comb. Theory B* **67**, 111–151 (1996).
- Dorogovtsev, S. N., Goltsev, A. V. & Mendes, J. F. F.  $k$ -core organization of complex networks. *Phys. Rev. Lett.* **96**, 040601 (2006).
- Carmi, S., Havlin, S., Kirkpatrick, S., Shavitt, Y. & Shir, E. A model of Internet topology using  $k$ -shell decomposition. *Proc. Natl Acad. Sci. USA* **104**, 11150–11154 (2007).
- Alvarez-Hamelin, J. I., Dall’Asta, L., Barrat, A. & Vespignani, A.  $k$ -core decomposition of the Internet graphs: hierarchies, self-similarity and measurement biases. *Netw. Heterog. Media* **3**, 371 (2008).
- Kitsak, M. et al. Identification of influential spreaders in complex networks. *Nat. Phys.* **6**, 888–893 (2010).
- Hagmann, P. et al. Mapping the structural core of human cerebral cortex. *PLoS Biol.* **6**, e159 (2008).
- Morone, F., Burleson-Lesser, K., Vinutha, H. A., Sastry, S. & Makse, H. A. The jamming transition is a  $k$ -core percolation transition. Preprint at <https://arXiv.org/abs/1804.07804> (2018).
- May, R. M. Mutualistic interactions among species. *Nature* **296**, 803–804 (1982).
- Holland, J. N., DeAngelis, D. L. & Bronstein, J. L. Population dynamics and mutualism: functional responses of benefits and costs. *Am. Nat.* **159**, 231–244 (2002).
- Bastolla, U. et al. The architecture of mutualistic networks minimizes competition and increases biodiversity. *Nature* **458**, 1018–1020 (2009).
- Thebault, E. & Fontaine, C. Stability of ecological communities and the architecture of mutualistic and trophic networks. *Science* **329**, 853–856 (2010).
- Alon, U. *An Introduction to Systems Biology: Design Principles of Biological Circuits* (CRC Press, Boca Raton, 2006).
- Amit, D. J. *Modeling Brain Function: The World of Attractor Neural Networks* (Cambridge Univ. Press, Cambridge, 1989).
- Sompolinsky, H., Crisanti, A. & Sommers, H. J. Chaos in random neural networks. *Phys. Rev. Lett.* **61**, 259–262 (1988).
- Okuyama, T. & Holland, J. N. Network structural properties mediate the stability of mutualistic communities. *Ecol. Lett.* **11**, 208–216 (2008).
- Arroyo, M. T. K., Primack, R. B. & Armesto, J. J. Community studies in pollination ecology in the high temperate Andes of Central Chile. I. Pollination mechanisms and altitudinal variation. *Amer. J. Bot.* **69**, 82–97 (1982).
- May, R. M. Simple mathematical models with very complicated dynamics. *Nature* **261**, 459–467 (1976).
- Shen-Orr, S. S., Milo, R., Mangan, S. & Alon, U. Network motifs in the transcriptional regulation network of *Escherichia coli*. *Nat. Genet.* **31**, 64–68 (2002).

33. Kauffman, S. A. *The Origins of Order: Self-organization and Selection in Evolution* (Oxford Univ. Press, New York, 1993).
34. Glass, L. & Kauffman, S. A. The logical analysis of continuous, non-linear biochemical control networks. *J. Theor. Biol.* **38**, 103–129 (1973).
35. Rohr, R. P., Saavedra, S. & Bascompte, J. On the structural stability of mutualistic systems. *Science* **345**, 1253497 (2014).
36. Bascompte, J., Jordano, P., Melián, C. J. & Olesen, J. M. The nested assembly of plant-animal mutualistic networks. *Proc. Natl Acad. Sci. USA* **100**, 9383–9387 (2003).
37. Staniczenko, P. P. A., Kopp, J. C. & Allesina, S. The ghost of nestedness in ecological networks. *Nat. Commun.* **4**, 1931 (2013).
38. Bickle, A. Cores and shells of graphs. *Math. Bohem.* **138**, 43–59 (2013).
39. Berry, D. & Widder, S. Deciphering microbial interactions and detecting keystone species with co-occurrence networks. *Front. Microbiol.* **5**, 00219 (2014).
40. Morone, F. & Makse, H. A. Influence maximization in complex networks through optimal percolation. *Nature* **524**, 65–68 (2015).
41. Bucci, V., Bradde, S., Biroli, G. & Xavier, J. B. Social interaction, noise and antibiotic-mediated switches in the intestinal microbiota. *PLoS. Comput. Biol.* **8**, e1002497 (2012).
42. Kato, M., Makutani, T., Inoue, T. & Itino, T. Insect–flower relationship in the primary beech forest of Ashu, Kyoto: an overview of the flowering phenology and seasonal pattern of insect visits. *Contr. Biol. Lab. Kyoto Univ.* **27**, 309–375 (1990).

## Acknowledgements

Research was sponsored by NSF-IIS 1515022, NIH-NIBIB R01EB022720, NIH-NCI U54CA137788/U54CA132378 and Army Research Laboratory under Cooperative Agreement W911NF-09-2-0053 (ARL Network Science CTA). We are grateful to S. Alarcón for discussions.

## Author contributions

All authors contributed equally to all parts of the study.

## Competing interests

The authors declare no competing interests.

## Additional information

**Supplementary information** is available for this paper at <https://doi.org/10.1038/s41567-018-0304-8>.

**Reprints and permissions information** is available at [www.nature.com/reprints](http://www.nature.com/reprints).

**Correspondence and requests for materials** should be addressed to H.A.M.

**Publisher's note:** Springer Nature remains neutral with regard to jurisdictional claims in published maps and institutional affiliations.

© The Author(s), under exclusive licence to Springer Nature Limited 2018

## Methods

**Numerical integration.** In general, the interaction strengths between species in ecological networks are weighted and directed<sup>9</sup> (that is,  $\gamma_{ij} \neq \gamma_{ji}$ ), meaning that the effect of species  $i$  on species  $j$  is different from the effect of species  $j$  on species  $i$ , and also the interaction strengths are all different (Fig. 2a). This heterogeneity is relevant to the stability of coupled systems and it is important to study their relevancy to the determination of the tipping point. Therefore, we study the influence of weighted interactions on the location of the tipping point of the dynamical system given by equation (1).

For our numerical investigation, we characterize the weights of the interactions  $\gamma_{ij}$  by a probability distribution with mean value  $\gamma$  and width  $\Delta$ . Following<sup>23,25</sup>, we take  $\gamma_{ij}$  as i.i.d. random variables drawn from the uniform distribution  $P(\gamma_{ij}) = \frac{1}{2\Delta}$ , if  $\gamma - \Delta \leq \gamma_{ij} \leq \gamma + \Delta$ , and zero otherwise (Fig. 2a). We systematically study how the width of the distribution of interactions affects the solution of the problem (see Fig. 2b–f and Supplementary Section III for details).

We simulate the dynamics of directed and weighted mutualistic systems spanning a large range of parameters across almost two orders of magnitude in the death rate:  $d = 0.05$  to  $d = 4$  (the range of values of  $d$  used in the simulations covers beyond the range of field measurements<sup>23,25</sup>, which are typically within  $d = 0.1$ – $0.3$ ). We use different uniform distributions  $P(\gamma_{ij})$  parametrized by the width  $\Delta$ , spanning from  $\Delta = 0$  (corresponding to a unweighted system where all interactions are equal,  $\gamma_{ij} = \gamma$ ) to a system with the widest possible distribution of  $\gamma_{ij}$  (corresponding to the maximum width  $\Delta_{\max}$  allowed by the condition  $\Delta < \gamma$ , which is necessary for a mutualistic system where all interactions are positive,  $\gamma_{ij} > 0$ ). The self-limitation parameter  $s$  can be absorbed into the definition of  $d$  and  $\gamma_{ij}$  by dividing both parameters; therefore, without loss of generality, we fix  $s = 1$  in the simulations—this has the sole effect of changing the unit of measure of the average density by a factor  $1/s$ .

A feasible, stable and non-zero solution is found for  $K_\gamma < K_c$ . By feasible, it is understood that the densities  $x_i^*$  must be non-negative (that is,  $x_i \geq 0$ ) for all species  $i$  (refs 5,6,24,25). A necessary (but not sufficient) condition for the survival of species, and thus for the existence of a feasible nontrivial fixed point  $\mathbf{x}^* \neq \mathbf{0}$ , is that  $d < \gamma$ . This means that the maximal mutualistic benefit supply of growth factors provided by the interacting species, corresponding to the interaction strength  $\gamma$  of the nonlinear interaction term, must be larger than the death rate  $d$ .

A comparison performed in Fig. 2b–f (Fig. 2g shows the case  $\Delta = 0$ ) between the numerical solutions for a wide range of parameters and the logic approximation (black curve) shows a good agreement between the theoretical and numerical solution. Figure 2h plots a comparison between the predicted tipping point for this network  $k_{\text{core}}^{\max} = 4$  and the numerical solution, showing that the logic approximation agrees well with the numerical solution for realistic values of death rates  $d \in [0.1$ – $0.3]$ <sup>23,25</sup> (Supplementary Section VI elaborates on these results). We estimate that real ecosystems can be approximated by  $\Delta = 0$  (that is, the variability in the interaction term does not noticeably affect the tipping point location for realistic values of the death rate). Second, the  $n = 1$  interaction term can be replaced by the logic approximation. These two approximations allow one to obtain the exact solution of the fixed-point equations.

In Supplementary Section VI C,D we also consider more realistic distributions, such as the right-skewed distributions found empirically in Bascompte et al.<sup>9</sup>. We integrate numerically equation (1) via a fourth-order Runge–Kutta algorithm until the system reaches the fixed point (the simulation procedure is similar to the one explained in Supplementary Section III with  $P(\gamma_{ij})$  empirically measured in ref. <sup>9</sup>).

## Data availability

Data that support the findings of this study are publicly available at the Interaction Web Database at <https://www.nceas.ucsb.edu/interactionweb/>.